Monte Carlo Analysis of Wall Erosion and Direct Contact Heat Transfer by Impinging Two-Phase Jets

Amir Kitron,* Tov Elperin,† and Abraham Tamir‡
Ben Gurion University of the Negev, Beer-Sheva, Israel

A stochastic model, based on the Boltzmann kinetic equation, is suggested for describing the flow of solid particles in impinging two-phase jets. The model is valid for highly nonequilibrium dilute impinging flows in which the inertia of the particles is very high and dynamic coupling with the fluid is low. The model includes the effects of interparticle collisions and is employed for predicting wall erosion rates by particle impacts and direct contact heat transfer from a surface by the colliding particles. A Monte Carlo simulation procedure is proposed, and numerical results are presented. The numerical results confirm experimental observations on reduced erosion rates caused by surface shielding by rebounding particles. Laminar and turbulent flow patterns as well as brittle and ductile erosion modes are studied. The results indicate, in accordance with experimental observations, an increase in the shielding effect when increasing the particles' volume fraction, elasticity, and angle of incidence and decreasing the particles' diameter. Interparticle collisions are shown to increase ductile erosion rates and decrease brittle erosion rates. In heat transfer from a wall, at low particle concentrations, interparticle collisions improve the heat transfer resulting from decreased impact velocities, but at higher concentrations the heat transferred by particles decreases because of surface shielding by rebounding particles.

Nomenclature

A_{12} = maximal contact area between colliding particles
C_p = particle heat capacity
d_p = particle diameter
$f_i(\boldsymbol{v},\boldsymbol{r},t)$ = distribution function for particles of type i
E = modulus of elasticity
$\boldsymbol{F}$ = external force acting on particles
h = cell dimension
m = particle mass
$\boldsymbol{n}$ = unit normal vector at the collision surface
N_{mk} = number of particles of type k in cell m
Nu = Nusselt number
Re = Reynolds number
$S_i(\boldsymbol{v},\boldsymbol{r},t)$ = external source term for particles of type i
t = time
Δt_m = simulation time interval
T = temperature
u' = turbulent gas velocity
U = gas velocity
$\boldsymbol{v}$ = particle velocity
V_m = volume of cell m
W_e = (volume eroded)/(incident particle mass)
β = particle volume fraction
γ = incidence angle
δ = mean spacing between particles
ε = restitution coefficient
$\varepsilon_b,\varepsilon_d$ = stress required to remove surface material in brittle and ductile erosion modes, respectively
η = coefficient of solid friction
η_b,η_d = mechanical efficiency of impact in brittle and ductile modes, respectively
κ_p = particle thermal conductivity
λ = mean free path between collisions
μ_g = gas viscosity
ν = Poisson ratio
ν_i = collision frequency for a single particle of type i
ρ = density
σ_{ij} = cross section for collision between particles of types i and j
σ = yield strength of eroded material
τ = unit vector normal to $\boldsymbol{n}$ on the plane of the relative velocity and $\boldsymbol{n}$
τ_h = hydrodynamical relaxation time
τ_λ = Lagrangian time scale for a turbulent fluid

Subscripts

b = brittle
d = ductile
g = gas
0 = in jet's entrance
p = particle
r = radial
w = in collision with wall
z = axial

Received Oct. 2, 1987; revision received May 11, 1988.

*Ph.D. Student, Department of Chemical Engineering.
†Senior Lecturer, Department of Mechanical Engineering and Pearlstone Center for Aeronautical Engineering Studies.
‡Professor, Department of Chemical Engineering.

I. Introduction

EROSION by solid particles carried by a gas causes grave damage in pneumatic transport systems, turbine blades exposed to dust or coal, and aerospace vehicles. Although several studies have described the surface erosion caused by aerodynamically entrained solid particles by considering independent particle impacts,[1-4] no predictions are available for the long-known effect of particle interactions on erosion rates. Smeltzer et al.[5] noted a reduction in erosion rate per particle flux when the particle concentration increased. This trend also has been noted in Tilly's review,[6] describing a typical reduction of erosion rate by 50% for a fortyfold increase in concentration. Uumois and Kleis[7] suggested that experiments that failed to identify this concentration effect involved narrow limits of particle concentrations or else were carried out within the ranges of concentration where the concentration effect is negligible. A similar trend has been observed in the erosion of a blunt body transversing a rain field.[8] This behavior may be attributed to interparticle collisions. The attacking particles, before impinging on the surface, must penetrate a

"cloud" of rebounding particles and debris. Thus, an attacking particle's impact velocity is decreased, and its direction is changed, thereby possibly preventing its collision with the surface. Therefore, rebounding particles near the eroded surface may be regarded as shielding it, in a manner similar to debris shielding ascribed to the high-speed erosion of bodies in a rain field.[8] Moreover, experimental investigations of the brittle erosion mode have indicated that maximal surface erosion by particle-laden jets did not occur at an incidence angle of 90 deg, although the brittle erosion by a single particle should be maximal at this angle; it has been surmised that at this angle there is considerable interference of incident particles with rebounding particles, hence, the reduced erosion.[9]

In addition to the particles' incidence angle, the following parameters reportedly have increased the effect of particle concentration on the erosion rates[7]: the impact velocity, strength of the abrasive particle, and particle size.

A further difficulty in erosion modeling lies in the need to relate the erosion to gas-particle interactions.[2,6] Empirical erosion rate expressions often implicitly include gas influences, such as deceleration of incident particles, turbulence effects, etc.

Interparticle and gas-particle effects in the impingement of a particle-laden jet on a surface are also relevant to heat transfer processes. It has been suggested that solid particles could enhance the heat removal rate from a wall by crossing the gas boundary layer adjacent to the wall and thus facilitate the heat transfer to the bulk of the gas.[10] Interparticle collisions in such a process may be expected to affect the heat transfer efficiency by conducting heat to each other, changing the impact durations, and shielding the surface.

The aim of this research is to develop a stochastic model and provide a Monte Carlo simulation method for predicting the erosion and heat transfer caused by a gas-solids suspension jet impinging on a surface, taking into account interparticle collisions. The model is valid for highly nonequilibrium dilute impinging flows in which the inertia of the particles is very high and dynamic coupling with the fluid is low.

II. Stochastic Model for Particle Collisions in Flowing Gas-Solids Suspensions

Collisions between particles are caused by differences in particle velocities. In many cases, these collisions can be described as a stochastic phenomenon. The differences in velocities relevant to erosion of and heat transfer from surfaces arise particularly from the interaction of incident particles with particles stuck to or rebounding from a surface, but also may arise from differences in response to a flowfield by particles of different size or mass, field shear, stochastic effects in the flowfield, such as fluid turbulence and Brownian motion, and random excitations of the flowfield such as wakes and sonic waves.

An analogy between particle collisions in suspensions and molecular collisions described in the kinetic theory of gases enables the application of the Boltzmann equation for the solid particles, as first suggested by Pai.[11] Consider the flow of a gas carrying spherical solid particles of uniform sizes under the following assumptions. Only binary collisions between particles are considered, and the duration of collision is assumed to be negligibly small. The latter assumption allows one to neglect hydrodynamical effects during collisions and is valid when the ratio of the solid particle's density ρ_p to the gas density ρ_g is much greater than unity, i.e., $\rho_p/\rho_g \gg 1$.[12] Furthermore, particle collisions are assumed to involve only pairs of particles having uncorrelated precollision velocities. The foregoing assumptions are similar to those made in the derivation of the Boltzmann transport equation in gas dynamics.[13]

The accepted model requires that the deviation in the trajectories of colliding particles caused by hydrodynamical interaction, resulting in a reduction in collision rate,[14] be neglected.

The dynamics of binary interparticle collisions have been considered in detail by Jenkins and Savage[15] and Ogawa.[16] If we suppose that the unit vector $\boldsymbol{n}$, directed from the center of one particle to the center of the other particle in contact with it, is constant throughout the interparticle collision, the particle velocities normal to the plane of contact before and after the collision are related as

$$(\boldsymbol{v}_1' - \boldsymbol{v}_2') \cdot \boldsymbol{n} = -\varepsilon(\boldsymbol{v}_1 - \boldsymbol{v}_2) \cdot \boldsymbol{n} \tag{1}$$

where $\boldsymbol{v}$ is a linear velocity, 1 and 2 are particle indices, primes denote post-collision values, and ϵ $(0 < \epsilon < 1)$ is the restitution coefficient. The case of $\epsilon = 1$ corresponds to an elastic collision. The friction between colliding particles causes a reduction of the relative velocity in the direction tangent to the plane of collision:

$$(\boldsymbol{v}_1 - \boldsymbol{v}_2) \cdot \boldsymbol{\tau} - (\boldsymbol{v}_1' - \boldsymbol{v}_2') \cdot \boldsymbol{\tau} = \eta(1 + \varepsilon)(\boldsymbol{v}_1 - \boldsymbol{v}_2) \cdot \boldsymbol{n} \tag{2}$$

where η is the coefficient of solid friction and τ is a unit vector normal to $\boldsymbol{n}$, in a plane containing $\boldsymbol{n}$ and $\boldsymbol{v}_1 - \boldsymbol{v}_2$. Since friction cannot reverse the tangential component of the relative velocity, the aforementioned reduction is conditional on avoiding such a reversal.

According to these assumptions, a collision between two particles of masses m_α, α being a particle's index, results in the following particle linear velocities:

$$\boldsymbol{v}_\alpha' = \boldsymbol{v}_\alpha + (-1)^\alpha\left(\frac{\mu}{m_\alpha}\right)\{(1 + \varepsilon)[(\boldsymbol{v}_1 - \boldsymbol{v}_2) \cdot \boldsymbol{n}]\boldsymbol{n} + [(1 - R)(\boldsymbol{v}_1 - \boldsymbol{v}_2) \cdot \boldsymbol{\tau}]\boldsymbol{\tau}\} \tag{3}$$

where μ is the reduced mass given as

$$\mu = \frac{m_1 m_2}{(m_1 + m_2)} \tag{4}$$

and R is given as

$$R(\theta) = \begin{cases} 1 - \eta(1 + \varepsilon)\cot\theta & \text{if} \quad \theta^* \le \theta \le \frac{\pi}{2} \\ 1 & \text{if} \quad 0 \le \theta \le \theta^* \end{cases} \tag{5}$$

where

$$\theta = \cos^{-1}\left[\frac{\boldsymbol{n} \cdot (\boldsymbol{v}_1 - \boldsymbol{v}_2)}{|\boldsymbol{v}_1 - \boldsymbol{v}_2|}\right] \tag{6}$$

and

$$\theta^* = \tan^{-1}\eta(1 + \varepsilon) \tag{7}$$

The discontinuity in R arises from the foregoing stipulation that friction does not reverse the slip velocity between the particles.

If we apply this collision dynamics model and the assumptions just listed, the Boltzmann equation for the particle distribution function in a mixture of s particle types may be derived following the standard procedure,[13] yielding a set of coupled transport equations

$$\frac{\partial f_i(\boldsymbol{v},\boldsymbol{r},t)}{\partial t} + \nabla_{\boldsymbol{r}} \cdot [\boldsymbol{v} f_i(\boldsymbol{v},\boldsymbol{r},t)] + \nabla_{\boldsymbol{v}} \cdot \left[\frac{\boldsymbol{F} f_i(\boldsymbol{v},\boldsymbol{r},t)}{m_i}\right] = S_i(\boldsymbol{v},\boldsymbol{r},t) + \sum_{j=1}^{s} \int_{W_v} \int_0^{4\pi} [(\varepsilon J) f_j(\boldsymbol{v}',\boldsymbol{r},t) f_i(\boldsymbol{v}_1',\boldsymbol{r},t) - f_j(\boldsymbol{v},\boldsymbol{r},t) f_i(\boldsymbol{v}_1,\boldsymbol{r},t)] |\boldsymbol{v} - \boldsymbol{v}_1| \sigma_{ij} \, d\boldsymbol{v}_1 \, d\Omega/(4\pi) = S_i(\boldsymbol{v},\boldsymbol{r},t) + \boldsymbol{I}_i(f,f) \tag{8}$$

where $f_i = f_i(\boldsymbol{v},\boldsymbol{r},t)$ is the distribution function for particles of type i; $\boldsymbol{r}$ is a position vector, t the time; $\boldsymbol{F}/m$ the particle acceleration resulting from body forces and gas friction;

$S_i(\boldsymbol{v},\boldsymbol{r},t)$ the external source term for particles of type i; the velocities $\boldsymbol{v}'$ and $\boldsymbol{v}_1'$ are related to $\boldsymbol{v}$ and $\boldsymbol{v}_1$ by Eq. (3); σ_{ij} is the collision cross section, given as $\pi(d_i + d_j)^2/4$ for a collision between particles of types i and j; $d\Omega$ is the differential solid angle; W_v is the domain in the space of velocities. The (εJ) factor, appearing in the collision term $I_i(f,f)$, arises from the aforementioned inelasticity and friction in particle collisions, with J being the Jacobian of the transformation $(\boldsymbol{v}_i,\boldsymbol{v}_j) \rightarrow (\boldsymbol{v}_i',\boldsymbol{v}_j')$: $J = d\boldsymbol{v}_i'\, d\boldsymbol{v}_j'/(d\boldsymbol{v}_i\, d\boldsymbol{v}_j)$. Ogawa[16] eliminated the discontinuity in R by averaging it over θ, obtaining for uniform-size particles

$$J = \varepsilon R^2 \tag{9}$$

The value $J = 1$ corresponds to elastic, frictionless collisions. The terms appearing at the left-hand side of the Boltzmann equation describe the convective variations in $f_i(\boldsymbol{v},\boldsymbol{r},t)$ along the particle trajectories, whereas the $I_i(f,f)$ term describes the variation of the distribution function caused by binary collisions between particles, and the $S_i(\boldsymbol{v},\boldsymbol{r},t)$ term accounts for external particle sources or sinks. The distribution functions and external sources term are normalized as follows:

$$\int_{W_r}\int_{W_v} f_i(\boldsymbol{v},\boldsymbol{r},t)\, d\boldsymbol{r}\, d\boldsymbol{v} = N_i(t) \tag{10}$$

$$\int_{W_r}\int_{W_v} S_i(\boldsymbol{r},\boldsymbol{v},t)\, d\boldsymbol{r}\, d\boldsymbol{v} = \zeta_i(t) \tag{11}$$

where W_r is the system's volume, N_i is the number of particles of type i in the system, and ζ_i is the overall rate of change of N_i caused by external sources or sinks.

Since the foregoing set of nonlinear integro-differential transport equations is as yet beyond analytical solution, numerical simulation must be employed. Although Monte Carlo simulation methods have been used extensively to solve various rarefied gasdynamics problems, only a few attempts have been made to apply these methods to suspension flows. Recently, a stochastic model has been employed for the simulation of gas-solids suspension flows in impinging stream reactors, including laminar and turbulent pipe flows.[17]

This work provides a Monte Carlo method for simulating the erosion and heat transfer caused by a gas-solids suspension jet impinging on a surface. The considered suspension flow is appropriate to the presented system of transport equations, taking into account gas friction effects, spatial nonhomogeneity, and the size distribution among particles. Since the formation of debris is a rather complex process, depending on various impact parameters and material properties, it will be neglected. To simplify the treatment of heat-transfer processes, radiation effects are neglected; the validity of this assumption has been established for low flow Mach numbers and gas temperatures.[18]

III. Employment of the Monte Carlo Direct Simulation Method

In this work, the direct simulation Monte Carlo (DSMC) method, first suggested by Bird[19] for solving the Boltzmann equation appropriate to rarefied gasdynamics, is used for simulating solid particle flow in a gaseous suspension.

The key ideas of the DSMC method devised by Bird are 1) the uncoupling of molecular motions and collisions during a time step Δt_m, i.e., the use of the operator-splitting technique; 2) the simulation of molecular collisions by disregarding molecular position coordinates within spatial cells; and 3) the simulation of fewer particles than those in the real flow, while normalizing the collision cross section so that the collision rate is not changed. Assumption 1 is valid when Δt_m is smaller than the time between collisions and larger than the collision's duration, and assumption 2 is valid provided that the cell is so small that the spatial variation of flow variables in the cell is negligible. Idea 3 of the DSMC method is usually unnecessary for suspension flow because of relatively small particle number densities; its validity follows from the invariance of the Boltzmann equation (8) to the scaling transformation.

The following is an outline of the operator-splitting technique in Bird's method. Let $f_i^n(\boldsymbol{r},\boldsymbol{v})$ approximate the distribution function at the nth time step, i.e., at time $t = n \cdot \Delta t_m$. To obtain the solution $f_i^{n+1}(\boldsymbol{r},\boldsymbol{v})$ at the $(n+1)$th time step, we consider first the collisionless transport equation

$$\frac{\partial \Phi_i}{\partial t} + \nabla_r(\boldsymbol{v}\Phi_i) + \nabla_v\left(\frac{\boldsymbol{F}\Phi_i}{m}\right) = S_i(\mathbf{r},\mathbf{v},t) \tag{12}$$

with $f_i^n(\boldsymbol{r},\boldsymbol{v})$ accepted as the initial value. At the second stage, $f_i^{n+1}(\boldsymbol{r},\boldsymbol{v})$ is obtained by solving the system of homogeneous Boltzmann equations

$$\frac{\partial f_i^{n+1}}{\partial t} = I_i(f^{n+1}, f^{n+1}) \tag{13}$$

with the solution Φ_i obtained at the first stage as the initial value. The solution of these equations at time $(n+1)\Delta t_m$ is found by sampling binary collisions between particles, as next described. The overall solution is thus accurate to the first order in both time and spatial increments.

Under the assumptions listed in the foregoing formulation of the system of coupled transport equations and by employing Bird's first and second assumptions, the DSMC method for the flow of gas-solids suspension is described as follows. The flow system is divided into equal-volume cells. Simulated particles are distributed in the system, with their positions and velocities sampled from the initial distribution function. When a stationary system of transport equations is solved, the initial distribution function is chosen arbitrarily, and the stationary solution is obtained by relaxation techniques, i.e., as the long-time asymptotics of the nonstationary solution.

Particles are allowed to move in the system without colliding with each other for a time interval Δt_m, with their subsequent positions, velocities, and temperatures determined from the particle's equation of motion and the equation of heat transfer between the particle and the gas. Within the time interval Δt_m, a particle may encounter a boundary: either an open boundary, where particles exit from the system, or a surface, where the particle's velocity and temperature after the collision (taken to be negligibly short) are calculated according to the model adopted for the collision's dynamics, i.e., the elasticity and friction, and the expressions for heat transfer, described next. Upon each particle contact with a surface, the erosion and heat transferred during the contact are recorded using expressions for the impact of a single particle.

Following the collisionless flow, particles are allowed to collide with each other. Let $N_{m,k}$ be the number of particles of type k in cell m having a volume V_m. The total number of particles in cell m is

$$N_m = \sum_{k=1}^{s} N_{mk} \tag{14}$$

A pair of colliding particles of types i and j is sampled from the number of possible different pairs of particles of these types with probability $\sigma_{ij}v_{ij}/(\sigma_{ij}^*v_{ij}^*)$, where v_{ij} is the relative velocity between the particles and v_{ij}^* and σ_{ij}^* are the maximum relative velocity and collision cross section, respectively, between particles of types i and j in the cell. Particle velocities after collision are calculated from Eq. (3). A particle's temperature $T_{p,1}'$ following a collision is obtained, following Soo,[20,21] as

$$T_{p,1}' = T_{p,1} + (T_{p,2} - T_{p,1}) \cdot \left\{1 - \exp\left[\frac{-2(\kappa_{p1}\kappa_{p2})^{1/2} A_{12}\, \Delta t_{\text{col}}}{m_1 C_{p1}(d_1 d_2)^{1/2}}\right]\right\} \tag{15}$$

where T_p is the particle's temperature, $T_{p.2} - T_{p.1}$ the mean temperature difference between the colliding particles during the collision, κ_p the particle's thermal conductivity, C_p the particle's heat capacity, Δt_{col} the collision's duration, derived by Hertz and Rayleigh[22] as

$$\Delta t_{\text{col}} = 2.94 v_{12}^{-1/5} \cos\theta^{-3/5} \left[\frac{15\pi(1+\varepsilon)(m_1 m_2)(k_1+k_2)}{32(m_1+m_2)}\right]^{2/5} \cdot \left[\frac{2(d_1+d_2)}{d_1 d_2}\right]^{1/5} \tag{16}$$

where k is defined for each particle as

$$k = \frac{(1-\nu^2)}{\pi E} \tag{17}$$

ν being the Poisson ratio and E the modulus of elasticity, and A_{12} is the maximal contact area between particles

$$A_{12} = \pi 2^{-14/5} \left[\left(\frac{d_1}{d_2}\right)^{1/2} + \left(\frac{d_2}{d_1}\right)^{1/2}\right]^{-4/5} \left[\left(\frac{m_1}{m_2}\right)^{1/2} + \left(\frac{m_2}{m_1}\right)^{1/2}\right]^{-2/5} \cdot (\cos\theta)^{2/5} (d_1 d_2) \left[\frac{5\pi^2 v_{12}^2 (\rho_{p1}\rho_{p2})^{1/2}(k_1+k_2)(1+\varepsilon)}{2}\right]^{2/5} \tag{18}$$

where ρ_p is the particle's density.

After the collision, a time increment

$$\Delta t_{ij} = \frac{(1+\delta_{ij})V_m}{(N_{m,i} N_{m,j} v_{ij} \sigma_{ij})} \tag{19}$$

where $\delta_{ij} = 1$ if $i = j$ and $\delta_{ij} = 0$ otherwise, is added to a time counter T_{ij}^m for the collisions between particles of types i and j (both i, j and j, i collisions) in cell m. The combination of particle types having the smallest value of the local time counter T_{ij}^m is chosen for the next collision;[19] if all T_{ij}^m values are zero, the combination is randomly sampled. This procedure is repeated until all T_{ij}^m values exceed $(n+1)\Delta t_m$. The expected number of collisions in cell m during a time interval Δt_m between particles of types i and j is given as

$$M_{ij}^m = \frac{N_{m,i} N_{m,j} v_{ij} \Delta t_m \sigma_{ij}}{[(1+\delta_{ij})V_m]} = \alpha_{ij} \Delta t_m \tag{20}$$

where v_{ij} is the mean relative velocity between particles of types i and j. Bird[19] proved that the collision sampling just described allows one to preserve M^m in the case of uniform size particles. Similar arguments can be used to prove that the foregoing sampling method is valid for sampling collisions between particles of different types.

The process presented is repeated until a steady state is obtained when solving a stationary Boltzmann equation, whereas the solution of a nonstationary Boltzmann equation requires batch averaging of simulation runs.

The performance of the procedure depends on the choice of cell dimensions and value of the time increment Δt_m.

IV. Choice of Particle Properties

Consider a suspension of identical spherical particles. The mean spacing between such particles, when uniformly distributed in space, is given as

$$\delta = \left(\frac{\pi}{6\beta}\right)^{1/3} d \tag{21}$$

where β is the particles' average volume fraction in the system. An average mean free path between collisions can be estimated by elementary kinetic theory as

$$\lambda = \left(\frac{2^{1/2}\sigma \cdot 6\beta}{\pi d^3}\right)^{-1} = \frac{d}{(2^{1/2} \cdot 6\beta)} \tag{22}$$

The upper limit for the particle volume fraction $\beta_{\max}$ is given by the requirement that the mean free path between particle interactions be greater than the mean interparticle spacing δ.[21] Using the condition $\lambda = \delta$ and Eqs. (21) and (22) yields $\beta_{\max} = 0.055$. However, a more restrictive requirement on β is implied by the assumption that the suspension is sufficiently diluted, so that only binary interparticle collisions need be considered.

In the formulation of the transport equation (8), the deviation in trajectories of approaching particles caused by hydrodynamic forces was neglected. This deviation causes a reduction in particle collision rates by a factor known as the "fraction impacted" or collision efficiency. For spherical particles of diameter d_s moving with a gas at speed U and colliding with larger particles of diameter d_1, the fraction impacted may be neglected (according to data provided by Soo[21]) when

$$\frac{\rho_p U d_s^2}{18\mu_g d_1} > 100 \tag{23}$$

where μ_g is the gas viscosity. For solid particles flowing in a gas, the small gas viscosities and high particle densities relative to the gas render the fraction impacted negligible, unless particle size or velocity are very small.

In order to examine the validity of neglecting the collision duration, consider the expression provided by Soo[9] for the duration of a collision between two identical spheres

$$\Delta t_{\text{col}} = 2.94 v_{12}^{-1/5} \cos\theta^{-3/5} d \left[\frac{5(1+\varepsilon)\rho_p(1-\nu^2)}{16E}\right]^{2/5} \tag{24}$$

The hydrodynamical relaxation time for Stoke's law is

$$\tau_h = \frac{\rho_p d^2}{18\mu_g} \tag{25}$$

According to Eqs. (20) and (22), the collision frequency for a single particle of type i is given as

$$\nu_i = \sum_{j=1}^{s} \pi(d_i + d_j)^2 v_{ij} \left(\frac{6\beta}{\pi d_j^3}\right) \Big/ 4 \tag{26}$$

For characteristic values of $d = 0.001$ m, $\rho_p = 1000$ kg/m^3, $\beta = 0.001$, $\mu_{\text{air}} = 1.75 \times 10^{-5}$ kg/m/s, $\varepsilon = 0.8$, $\theta = 45$ deg., $v_{12} = 10$ m/s, $\nu = 0.4$, and $E = 5 \times 10^9$ Pa, one obtains $\Delta t_{\text{col}} = 3.5 \times 10^{-6}$ s, $\tau_h = 3.2$ s, and $1/\nu_i = 1.7 \times 10^{-5}$ s. Thus, $1/\nu_i \sim \tau_h > \Delta t_{\text{col}}$, i.e., the collision duration can be neglected.

A certain restriction may arise concerning the relation between the hydrodynamical relaxation time τ_h and the mean time between collisions $1/\nu_i$. The assumption that colliding particles have uncorrelated velocities, necessary for the derivation of the transport equation (8), is valid for gas dynamics because of the high rate of collisions between molecules. Since suspension flow involves much fewer interparticle collisions than gas flow, the hydrodynamical dampening of postcollision velocities should be strong enough to prevent such a correlation. However, if the hydrodynamical relaxation occurs too quickly, particles have small slip velocities relative to the gas, so that their velocities are highly correlated to the gas velocity at the location of the collision. The latter conclusion is equivalent to the requirement that the particles' self-collision Knudsen number $Kn_c = \lambda/D = d/(2^{1/2} 6\beta D)$, where D is a characteristic macroscopic length, must not considerably exceed the Knudsen number for collisions of particles with gas molecules, $Kn_h = \tau_h U/D$, where U is a characteristic flow velocity. Particularly, in cases where $Kn_h \ll Kn_c$, the effect of interparticle collisions is insignificant, since the particles take up the gas velocity instantly.

V. Choice of Cells Dimensions

Bird[19] set a cell's dimension h in a direction across which

particle concentrations and average velocities vary, as

$$h < \frac{\lambda}{3} \tag{27}$$

Still, an upper limit for h, which normally does not arise for gas molecules, is given by the stipulation that h be much greater than d (at least by one order of magnitude) so that calculating collisions only within cells is permissible. A general limitation for h is that it should be small enough to allow an analysis of variations in the space of flow variables with sufficient accuracy, while large enough to avoid long calculation times.

VI. Choice of Time Increments

Bird[19] suggested taking Δt_m smaller than $1/v_i$, so as to validate the uncoupling of the collisions between particles from their collisionless motion. When different particle sizes are considered, Δt_m should be taken smaller than the shortest estimated $1/v_i$.

It should be noted that the stability of the explicit two-stage operator splitting procedure just described requires that the time increment and cell size satisfy the Courant–Friedrichs–Lewy condition, whereby

$$\Delta t_m < \frac{h}{v^*} \tag{28}$$

where v^* is a characteristic particle velocity. This condition is consistent with Eqs. (22) and (26) for λ and v_i and Bird's requirement that $\Delta t_m < 1/v_i$.

VII. Equation of Collisionless Particle Motion

When only fluid drag acts on particles during Δt_m, a particle's trajectory is calculated by integrating the ordinary differential equation

$$\frac{\mathrm{d}^2 \boldsymbol{r}}{\mathrm{d}t^2} = 0.75 C_D \left[\frac{\rho_g}{\rho_p d_p}\right] |\boldsymbol{U} - \boldsymbol{v}|(\boldsymbol{U} - \boldsymbol{v}) \tag{29}$$

where $\boldsymbol{U}$ is the gas velocity at $\boldsymbol{r}$ and C_D; the standard drag curve for a single spherical particle is given by Clift et al.[23] as

$$C_D = \frac{3}{16} + \frac{24}{Re_p} \qquad 0 < Re_p < 0.01$$

$$\log\left(\frac{C_D Re_p}{24} - 1\right) = -0.881 + 0.82 \log(Re_p) - 0.05[\log(Re_p)]^2 \qquad 0.01 < Re_p < 20$$

$$\log\left(\frac{C_D Re_p}{24} - 1\right) = -0.7133 + 0.6305 \log(Re_p) \qquad 20 < Re_p < 260$$

$$\log(C_D) = 1.6435 - 1.1242 \log(Re_p) + 0.1558[\log(Re_p)]^2 \qquad 260 < Re_p < 1500$$

$$\log(C_D) = -2.4571 + 2.5558 \log(Re_p) - 0.9295[\log(Re_p)]^2 + 0.1049[\log(Re_p)]^3 \qquad 1500 < Re_p < 1.2 \times 10^4$$

$$\log(C_D) = -1.9181 + 0.637 \log(Re_p) - 0.0636[\log(Re_p)]^2 \qquad 1.2 \times 10^4 < Re_p < 4.4 \times 10^4$$

$$\log(C_D) = -4.339 + 1.5809 \log(Re_p) - 0.1546[\log(Re_p)]^2 \qquad 4.4 \times 10^4 < Re_p < 3.38 \times 10^5$$

$$C_D = 29.78 - 5.3 \log(Re_p) \qquad 3.38 \times 10^5 < Re_p < 4.03 \times 10^5$$

$$C_D = -0.49 + 0.1 \log(Re_p) \qquad 4.03 \times 10^5 < Re_p < 10^6 \tag{30}$$

where

$$Re_p = \rho_g d_p |\boldsymbol{U} - \boldsymbol{v}|/\mu_g \tag{31}$$

The lift forces acting on the particles because of gas shear (Saffman force, etc.) are neglected, since, for particles in a stream impinging on a surface, the drag in the direction of the lift force is usually dominant.

The particle's temperature change caused by heat transfer to the isothermal gas is calculated by assuming that the temperature within the particle is uniform. Then, the particle's temperature is found from the heat conduction equation

$$mC_p\left(\frac{\mathrm{d}T_p}{\mathrm{d}t}\right) = \kappa_g Nu \pi d(T_g - T_p) \tag{32}$$

where T_p and T_g are the particle and gas temperatures, respectively; κ_g is the gas thermal conductivity, and Nu is the Nusselt number for heat conduction and forced convection from the particle to the air, given as[18]

$$Nu = \begin{cases} 1 + (1 + Re_p)^{1/3} & 0 < Re_p < 3 \\ 1 + (1 + 0.70 Re_p)^{1/3} Re_p^{0.077} & 3 < Re_p < 100 \\ 1 + 0.6777 Re_p^{0.47} & 100 < Re_p < 4000 \\ 1 + 0.272\ Re_p^{0.58} & 4000 < Re_p < 10^6 \end{cases} \tag{33}$$

The ratio of the characteristic time for internal temperature equalization to the heat-transfer relaxation time defined by Eq. (32) is κ_g/κ_p.[24] This ratio is of the order of 10^{-4} for metal particles and 10^{-1} for sand particles in air. Thus, the assumption whereby the temperature distribution within the particles is uniform is valid. The radiation heat transfer between the gas and particles also may be neglected when the gas and particle temperatures are sufficiently low.[18] Since the suspension is dilute, the changes in gas temperatures because of heat transferred from the particles may be neglected, i.e., only direct-contact heat transfer is considered.

VIII. Surface Erosion and Heat Transfer by an Impacting Particle

Several phenomenological models have been proposed for analyzing the erosion of a surface by impacting particles.[9,21,25 28] All of these models use the correlations for the erosion by single-particle impact as a function of the attack angle, particle velocity, size, and mechanical properties of the particles and eroded surface. The effect of increased erosion rates caused by multiple impacts by rebounding particles was studied by Grant and Tabakoff.[26] The stochastic model and the Monte Carlo procedure they employed essentially differ from those developed in this work, since they do not take account of interparticle collisions. Soo[9,21] developed a model for the erosion of and heat transfer from surfaces by colliding solid particles. Soo's model for erosion is employed here rather than other models, since the latter are more empirical and may thus implicitly include interparticle and aerodynamic effects. Two basic erosion modes are considered. In the ductile erosion mode, which is usually dominant for metal targets, the erosion mechanism is the cutting or machining of the surface by a friction force. Erosion occurs only when the stress caused by this force exceeds the yield strength of the eroded material σ_d. Experiments indicate that the ductile mode is characterized by maximal erosion at incidence angles usually in the range of 20–30 deg. In the ductile erosion mode, the volume loss caused by erosion in the impact of a particle of velocity v and incidence angle γ is given by

$$w_d = \eta_d \left[\varphi_d \frac{P_d}{A_w} - \sigma_d \right] v \cos\gamma \frac{A_w \Delta t_w}{\varepsilon_d} \quad \text{for} \quad \varphi_d \frac{P_d}{A_w} > \sigma_d$$
$$0 \qquad \text{otherwise} \tag{34}$$

where η_d is a mechanical efficiency of impact, including the effects of gliding, scattering, and lifting of particles by the gas; φ_d corrects the nonsphericity of the actual particles, stress concentration at sharp edges, roughness of the surface impacted, and nonspecular reflection from an actual surface; P_d is the cutting force, determined from the impulse

$$P_d \Delta t_w = \eta_w 2.94 \left(\frac{5}{16}\right) mv(1+\varepsilon_w) \tag{35}$$

where Δt_w is the collision's duration, η_w and ε_w are the coefficients of friction and restitution in a particle-wall collision; A_w is the maximal contact area in the particle-wall collision, its product with Δt_w being determined from expressions (16) and (18) with $d_2/d_1 \to \infty$:

$$A_w \Delta t_w = (2.94)\left(\frac{3}{4}\right) 2^{-8/5} m \times \left[5\pi^2 \rho_p v^2 (k_p + k_w) \frac{(1+\varepsilon_w)}{2} \right]^{4/5} \cdot \frac{(\sin\gamma)^{-1/5}}{v\rho_p} \tag{36}$$

where k_w is the k value [expression(17)] corresponding to the surface's properties; ε_d is the stress required to remove surface material and is related to σ_d.

The brittle erosion mode is typical of glass and ceramics. It is characterized by an increase in erosion rate with the incidence angle. The brittle erosion proceeds by cracking the surface by fatigue and surface failure resulting from a normal compression force. The erosion occurs when the normal stress exceeds an impact yield strength σ_b. For the brittle erosion mode, the volume loss upon a single impact is

$$W_b = \eta_b \left[\varphi_b \frac{P_b}{A_w} - \sigma_b \right] v \sin\gamma \frac{A_w \Delta t_w}{\varepsilon_b} \quad \text{for} \quad \varphi_b \frac{P_b}{A_w} > \sigma_b$$
$$0 \qquad \text{otherwise} \tag{37}$$

where η_b, φ_b, and ε_b have an analogous meaning to the corresponding parameters in Eq. (29) and the force P_b is determined as

$$P_b \Delta t_w = 2.94 \left(\frac{5}{16}\right) mv(1+\varepsilon_w) \tag{38}$$

The foregoing erosion expressions are appropriate for metals, alloys, and ceramics. In such materials, the erosion process is the result of a combined effect of the brittle and ductile modes. These expressions are not, however, appropriate for rubber and some plastics, which may be penetrated by impacting particles and therefore involve different effects of a particle's concentration on the erosion rates.[7]

The change in particle temperature following the collision is given as[9]

$$T_p' = T_w + (T_p - T_w)\left\{ 1 - \exp\left[-2(\kappa_p \kappa_w)^{1/2} A_w \frac{\Delta t_w}{(mC_p d)} \right] \right\} \tag{39}$$

where $T_p - T_w$ is the mean temperature difference between the particle and the wall during the collision, T_w the wall's temperature, and κ_w the wall's thermal conductivity. Thus, the heat transferred to the wall during the collision is

$$Q = mC_p(T_p - T_p') \tag{40}$$

The presented analysis of the heat transferred neglects the heating of the surface by colliding particles caused by modification of the gas flowfield near the surface and conversion of incident particle kinetic energy to thermal energy.[29] Although the effect on the gas flowfield might be justified for dilute suspensions, the loss of kinetic energy is a substantial factor that may cause heating by an amount far exceeding the heat conducted. The effect is reduced when the difference in temperature between the surface and particles increases and when the collisions are more elastic.

IX. Gas Flow Patterns in the Impinging Particle-Laden Jet

Several gas flow patterns may be considered in the impingement of a particle-laden jet on a wall. For instance, the erosion by noninteracting particles in a potential gas flow has been analyzed by Laitone.[1]

In this work, simple gas flow patterns will be considered, so as to study extreme effects of particle concentrations on wall erosion rates. The first flow pattern to be studied is an infinite plane jet, with a uniform velocity U_0, impinging on a surface perpendicularly, or else tilted by a small angle. Such a pattern is clearly unrealistic, but may crudely approximate the flow in the vicinity of a round jet core. The effects of gravity, lift forces, and gas radial motion are neglected; particles leave the system once their speed approaches zero. The advantage of this approach is the possibility of studying the effect of interparticle collisions separately from other factors. The simulation volume has open boundaries on the surfaces other than the eroded surface, which are taken to be specularly reflecting because of the symmetry of the infinite plane jet flow. The specularly reflecting boundaries condition implies that when a particle exits from the control volume, another particle with identical velocity enters this control volume. When the jet is tilted with respect to the surface, the tilting angle is kept small, since for higher tilting angle values, the rebounding particles are swept away from the eroded surface by the gaseous flow and the effect of surface screening by the cloud of rebounded particles is less pronounced.

The second gas flow pattern examined will be similar to the foregoing pattern, except that the gas velocity will be described as

$$U_z = U_0 + u_z' \tag{41}$$

$$U_r = u'_r \tag{42}$$

where U_z and U_r are the velocity in the axial (perpendicular to the surface) and radial directions, respectively, and u'_z and u'_r are the axial and radial turbulent velocity components, respectively. Also, u'_z and u'_r are assumed to be normally distributed random variables with zero means and standard deviations, chosen as characteristic values from experimental data on impinging turbulent particle-laden jets[29-31]

$$(\bar{u}'^2_z)^{1/2} = 0.10U_0 \tag{43}$$

$$(\bar{u}'^2_r)^{1/2} = 0.15U_0 \tag{44}$$

The motion of solid particles in the turbulent velocity field was treated by the method suggested by Yoshida and Masuda.[32] Turbulent velocity pulsations are assumed constant during the average lifetime of a turbulent eddy, estimated as the Lagrangian time scale of the turbulent gas flow

$$\tau_\lambda = \frac{\Lambda_g}{[(\bar{u}'_r)^2 + (\bar{u}'_z)^2]^{1/2}} \tag{45}$$

where τ_λ is the average time for fresh fluid to surround a large particle, or an average time for a very small particle to travel the minimal characteristic length of the turbulent velocity field, and the Lagrangian spatial integral scale Λ_g may be estimated as[34]

$$\Lambda_g = 0.075 \cdot 2.6\delta_{1/2} \tag{46}$$

where $\delta_{1/2}$ is the jet's half width, which may be assigned[33] a value in the order of 0.5 cm.

The assumption employed in the derivation of the Boltzmann equation, whereby the velocities of colliding particles are uncorrelated, does not seem justified for the uniform gas velocity jet, because of the high correlation expected between a particle's position and its velocity. This correlation may be expected to increase as the hydrodynamical relaxation time τ_h decreases. Nevertheless, the employment of the Monte Carlo simulation procedure may be justified in this case as a kind of a "molecular dynamics" simulation of an ensemble of a finite number of particles.

In the case of turbulent suspension flow, the assumption equivalent to "molecular chaos" in the formulation of the Boltzmann equation requires that 1) the turbulence of the suspending fluid be isotropic on the scale of the collision process and 2) particles be projected at each other from independently moving fluid elements. In the stochastic model just described, these requirements are implied by integrating the equation of collisionless motion (29) for different solid particles, using independent turbulent pulsation velocities. As discussed by Abrahamson,[35] condition 1 is likely to be met in industrial pipe flows of gases at sufficiently high Reynolds numbers, where the characteristic correlation length of the turbulent velocity field is much smaller than the particle's free path length and diameter. Condition 2 requires that the particle's hydrodynamical relaxation time τ_h be larger than τ_λ.

In both the potential-flow pattern and turbulent jet, the effects of the solid particles on the gas flow characteristics are neglected. This assumption is justified for the low particle loadings concerned.[36]

X. Results and Discussion

Simulation of surface erosion was performed for silica particles impacting on a steel surface (see material properties in Table 1 and using, following Soo's discussion,[9] $\eta_b = \eta_d = 0.5$, $\varphi_b = \varphi_d = 2$). For a representative collision between silica particles of the type considered ($d_p = 1$ mm, for $v_{12} = 300$ m/s, $\theta = 45$ deg, $\varepsilon = 1$), the duration of collision and the collision area may be estimated from Eqs. (16) and (18) as $\Delta t_{\text{col}} = 1.16 \times 10^{-6}$ s and $A_{12} = 1.3 \times 10^{-7}$ m^2.

The initial condition in the simulation was a control volume free of particles. The particles, having the same velocity U_0 as that of the gas stream, were fed continuously with a mass flow rate appropriate to the particles' inlet volume fraction, at a distance $L = 0.3$ m from the surface, in a cross section having a radius of 11 mm (or in the case that the jet incidence angle $\gamma_0 \neq 0$, in a square section, each side of it being 11 mm long, one side being parallel to the direction of incidence). The control volume was divided into 60 equal-volume cells.

In the idealized model of an infinite plane particle-laden jet just described, the mechanism for the particles' exit from the system is inadequate. The particles were found to concentrate near the wall and accumulate indefinitely in the control volume. The erosion rates in different conditions still could be compared to each other by comparing overall erosion per particles weight over equal time periods or for equal quantities of incident particles. For a volume fraction $\beta = 0.001$, a quantity of about 500 particles accumulated in the control volume after 20 simulation time intervals of duration $\Delta t = 5.6 \times 10^{-4}$ s.

In the calculations, the mechanical properties of silica particles, surface properties, and particle volume fractions were kept close to experimental values.[7] For silica particles with $U_0 = 150$ m/s, $\beta = 0.001$, and $d = 1$ mm eroding a steel surface, the calculated erosion rate (~ 3 g eroded/Kg particles) was about three times as large as corresponding experimental results.[7] This discrepancy between experimental and theoretical results may be considered quite tolerable in view of some very idealized conditions employed in the simulation, such as high particle residence times near the eroded surface due to the assumed infinitely large jet, uniform gas velocity profile throughout the jet, etc.

In Table 2, calculated values for the surface erosion in uniform velocity gas flow and homogeneous turbulent gas flow, isolating the effect of particle collisions (with various

Table 1 Solid material properties

	Silica	Steel	Aluminum
E, Pa	6.53×10^{10}	1.9×10^{11}	6.8×10^{10}
ρ, kg/m^3	2180	8020	2243
ν	0.17	0.3	0.34
C_p, J/(K)(Kg)	942	505	968
k, J/(K)(m)(s)	3.6	34	222
ε_b, Pa	—	1×10^{10}	—
ε_d, Pa	—	1×10^{9}	—
σ_b, Pa	—	3.0×10^{8}	—
σ_d, Pa	—	3.0×10^{8}	—

Table 2 Steel erosion by silica particles: effects of turbulence, interparticle collisions, and rebounding

	(Volume steel eroded)/(mass particles) $\times 10^7$			
	Uniform gas jet		Turbulent gas jet	
	Brittle	Ductile	Brittle	Ductile
With collisions and rebounding				
$\varepsilon = 0.5$, $\eta = 0.8$	29.0	7.7	21.5	8.0
$\varepsilon = 1.0$, $\eta = 0$	16.0	13.5		
$\varepsilon = 0$, $\eta = 0$	30.0	5.3		
$\varepsilon = 0$, $\eta = 1$	31.1	1.1		
No collisions, with rebounding	34.8	0	20.0	8.0
No collisions, no rebounding	28.0	0		

($d_p = 1$ mm, $U_0 = 300$ m/s, $\tau_\lambda = 9 \times 10^{-5}$s, $\epsilon_w = 0.5$, $\eta_w = 0.8$, $\beta = 0.001$, $\Delta t_m = 5.6 \times 10^{-4}$s, simulated time period = 0.0112 s, $\gamma_0 = 90$ deg).

collision parameters) and of particles' rebounding from the eroded surface, are presented. In the simulation without rebounding, particles were removed from the system on their first impact with the eroded surface, whereas otherwise, particles rebounding from the surface were subsequently carried back toward the surface by the gas stream and more erosion resulted. The increased erosion caused by rebounding is evident in Table 2, particularly for uniform flow; in turbulent flow, turbulent pulsations cause particles to be swayed in various directions, so that the first impacts cause less erosion than in uniform flow, and the effect of secondary impacts is mitigated.

A comparison between erosion rates obtained for uniform flow with and without interparticle collisions (Table 2, with rebounding) indicates that interparticle collisions caused brittle erosion to decrease and ductile erosion to increase. Apparently, interparticle collisions decrease the brittle erosion by shielding the surface and decreasing impact angles (from the initial stream impact angle $\gamma_0 = 90$ deg) and velocities, and cause an increase in ductile erosion because of this very decrease in impact angles [see the effect of γ in Eq. (34)]. The requirement that particles be diverted from their perpendicular course in order to cause ductile erosion also accounts for the zero ductile erosion obtained for uniform gas flow without interparticle collisions compared to the non-zero value obtained for turbulent flow without interparticle collisions.

The effect of the particle collision parameters ε and η may be assessed from Table 2 for uniform gas flow. As just noted, interparticle collisions caused the brittle erosion to decrease but increased the ductile erosion. The increase in the elasticity factor ε appears to result in a large increase in the ductile erosion, apparently because of its strong effect on the number of particles that scatter sideways in collisions. A change in the particle collision parameters can determine, as seen in Table 2, whether the overall erosion is greater or smaller than that in the absence of interparticle collisions. It has been reported[7] that the effect of particle concentration on the erosion rate is strongly dependent on the type of material constituting the particles; the effects of elasticity and friction in collisions may be one explanation for this dependence.

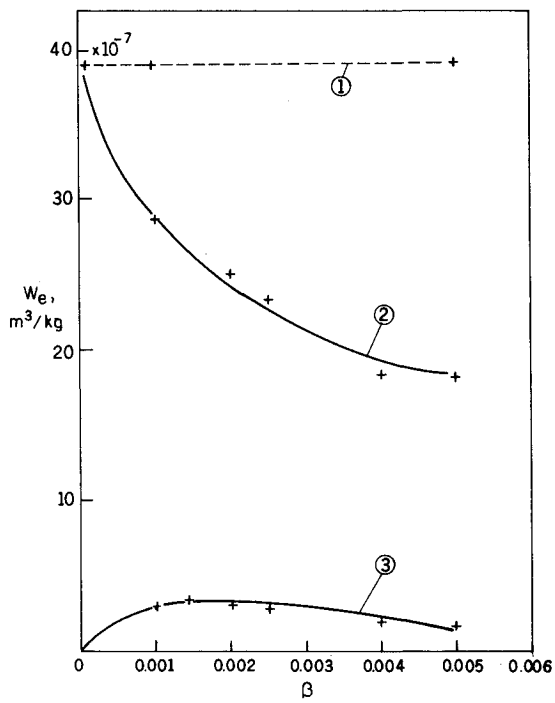

Fig. 1 Effect of particle inlet volume fraction on the erosion rate W_e = (volume eroded)/(incident particle mass) [steel eroded by 5.0×10^{-5} Kg of silica particles, $d_p = 1$ mm, $U_0 = 300$ m/s (uniform gas flow), $\gamma_0 = 90$ deg, $\varepsilon = \varepsilon_w = 0.5$, $\eta = \eta_w = 0.8$, 20 time intervals simulated]. ① Brittle erosion, no collisions. ② Brittle erosion, with collisions. ③ Ductile erosion, with collisions.

The effect of particle volume fraction in the incident particle-laden jet β is demonstrated in Fig. 1 for an equal incident mass of abrasive particles and equal erosion areas. It must be noted that under these conditions, a change in β corresponds to a change in the concentration defined by some authors[7] as a flux

$$\Psi = \frac{G}{A_t \cdot t} \tag{47}$$

where G is the mass of abrasive eroding a surface of area A_t during a time interval t; higher values of β require inversely proportional feeding times, so that Ψ increases proportionally to β. When interparticle collisions are not taken into account, the erosion is only in the brittle mode and is independent of the particles' concentration. When interparticle collisions are taken into account, an increase in β decreases the brittle erosion, from a value similar to that without particle interactions when $\beta \to 0$ up to some asymptotic value, and increases the ductile erosion from zero up to a maximum, beyond which it is decreased down to some asymptotic value. The effect of β may be analyzed by considering the average interparticle collision rate α for identical spherical particles, derived in elementary kinetic theory:[19]

$$\alpha = n^2 v_{12} \frac{\pi d^2}{2} \tag{48}$$

where n is the particle number density, v_{12} the average relative velocity between particles, and πd^2 the collision cross section. An increase in β results in an increased number density and hence, an increased interparticle collision rate. The aforementioned analysis of data in Table 2 has already revealed that interparticle collisions result in reduced brittle erosion rate and increased ductile erosion rate. In Fig. 1, the increase in collision rates seems to magnify these trends, except that ductile erosion is decreased beyond some concentrations. Apparently, at high particle concentrations, the more pronounced shielding mechanism prevents scattered particles from reaching the surface and thus decreases the ductile erosion.

Figure 1 again indicates that the increase in ductile erosion can cause, at low particle concentrations, an increase in overall erosion when increasing the particle concentration. Eventually, however, the overall erosion rate decreases with increased concentrations, up to some asymptotic value; the latter behavior is in accord with experimental observations.[7] The attaining of an asymptotic value may be accounted for by the attaining of a balance between the size and density of the screening particles "cloud" and the particles' influx, such that at greater influxes, the cloud becomes denser and thereby prevents an increase in erosion.

The effect of particle size on the effect of particle concentration on erosion rates is demonstrated in Fig. 2, for a constant particles' inlet volume fraction β. Since for all sizes the overall particles mass fed, the feeding duration, and eroded surface area were identical, the inlet mass flux Ψ was also constant. Expressions (34–37) indicate that the volume eroded/particle mass, for a single impact at a given velocity and angle, is independent of particle size. This indeed is the case indicated in Fig. 2 in the absence of interparticle collisions. When collisions are present, however, the brittle erosion rate is reduced, the strongest effect occurring for the smaller particle sizes. Uumois and Kleis[7] mention a similar trend, whereby the effect of particle concentration on the erosion rate is stronger for smaller particle sizes. This trend may be expected on the basis of Eq. (48); decreasing d by a factor y while maintaining β at a constant value implies an increase of n by y^3, so that the collision rate α is increased by y^4.

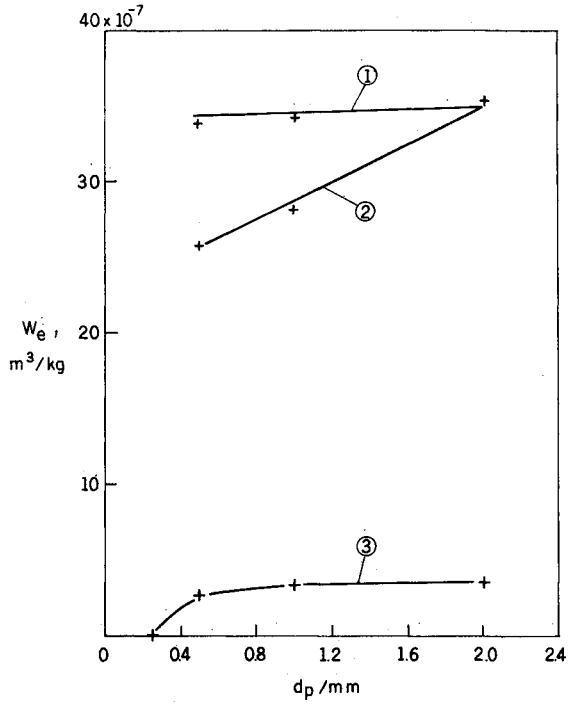

Fig. 2 Effect of particle diameter on the erosion rate W_e = (volume eroded)/(incident particle mass) [steel eroded by 2.5×10^{-5} Kg of silica particles, $\beta = 0.001$, $U_0 = 300$ m/s (uniform gas flow), $\varepsilon = \varepsilon_w = 0.5$, $\eta = \eta_w = 0.8$, $\gamma_0 = 90$ deg, simulated time duration = 5.4×10^{-3} s]. ① Brittle erosion, no collisions. ② Brittle erosion, with collisions. ③ Ductile erosion, with collisions.

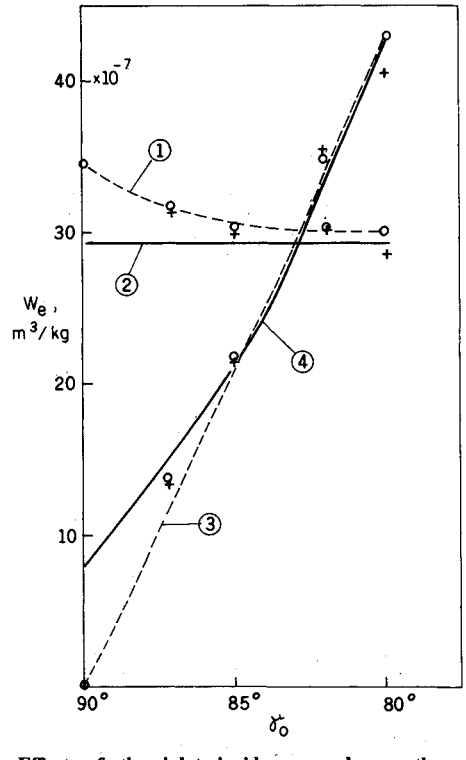

Fig. 3 Effect of the inlet incidence angle on the erosion rate W_e = (volume eroded)/(incident particle mass) [steel eroded by 5.0×10^{-5} Kg of silica particles, $d_p = 1$ mm, $U_0 = 300$ m/s (uniform gas flow), $\beta = 0.001$, $\varepsilon = \varepsilon_w = 0.5$, $\eta = \eta_w = 0.8$, 20 time intervals simulated]. ① Brittle erosion, no collisions. ② Brittle erosion, no collisions. ③ Ductile erosion, with collisions. ④ Ductile erosion, with collisions.

The effect of slightly varying the initial incidence angle γ_0 on the erosion is displayed in Fig. 3. As just mentioned, only small variations in γ_0 were studied, so as to investigate cases

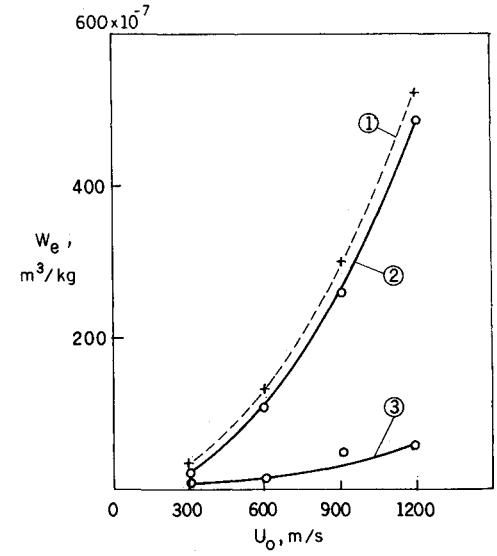

Fig. 4 Effect of gas velocity on the erosion rate W_e = (volume eroded)/(incident particle mass) [steel eroded by 5.0×10^{-5} Kg of silica particles, $d_p = 1$ mm, uniform gas flow, $\beta = 0.001$, $\varepsilon = \varepsilon_w = 0.5$, $\eta = \eta_w = 0.8$, 20 time intervals simulated, $\gamma_0 = 90$ deg]. ① Brittle erosion, no collisions. ② Brittle erosion, with collisions. ③ Ductile erosion, with collisions.

in which the effect of the particle concentraion on the erosion rate is pronounced. The geometrical setup of the simulated system was as described herein. When interparticle collisions are absent, decreasing γ_0 causes brittle erosion to decrease and ductile erosion to increase; these trends are well explained by the dependence of the erosion mechanisms on the impact angle [expressions (34–37)]. When interparticle collisions are taken into account, the brittle erosion rate does not change considerably with γ_0, and as γ_0 decreases, the brittle erosion seems independent of interparticle collisions. For $\gamma_0 = 90$ deg, the ductile erosion rate is, as noted previously, increased by interparticle collisions; decreasing γ_0, however, lessens the effect of these collisions over the ductile erosion rate. Apparently, in both erosion modes, the effect of interparticle collisions vanishes when the angle of attack is decreased from 90 deg, since the relative velocity between oncoming and rebounding particles is decreased [see the effect of v_{12} in Eq. (48)], and if the stream is not regarded as infinitely wide, the rebounding particles flow away from the oncoming particles. This trend is in accord with experimental results.[7,9].

The effect of the stream's initial velocity U_0 is demonstrated in Fig. 4 for constant particle volume fraction β and identical quantities of eroding particles. Although other authors have examined the effect of velocity on the concentration effect by preserving the flux Ψ rather than β,[7] in this work, β is preserved in order to maintain similar particle number densities, so that the effect of the relative velocity v_{12} in Eq. (48) may become more distinct.

In Fig. 4, the brittle erosion rate, in the absence of interparticle collisions, increases when the stream velocity increases. This may be explained by the strong dependence of the surface erosion on the impact velocity as seen in expressions (36–38). Similar trends appear for the brittle and ductile erosion rates with interparticle collisions taken into account, and again, the familiar decrease in brittle erosion and increase in ductile erosion with respect to the no-interaction condition are obtained. Unlike claims made elsewhere,[7] whereby a greater reduction in erosion rates due to interparticle collisions is obtained for higher velocities, so that the effect of particle concentration on the overall erosion rate is more prominent at higher velocities, in the calculated value this trend was not evident. The latter may also be expected on the basis of Eq. (48), since v_{12} is increased. Nevertheless, it appears that at higher velocities, the particles are slowed

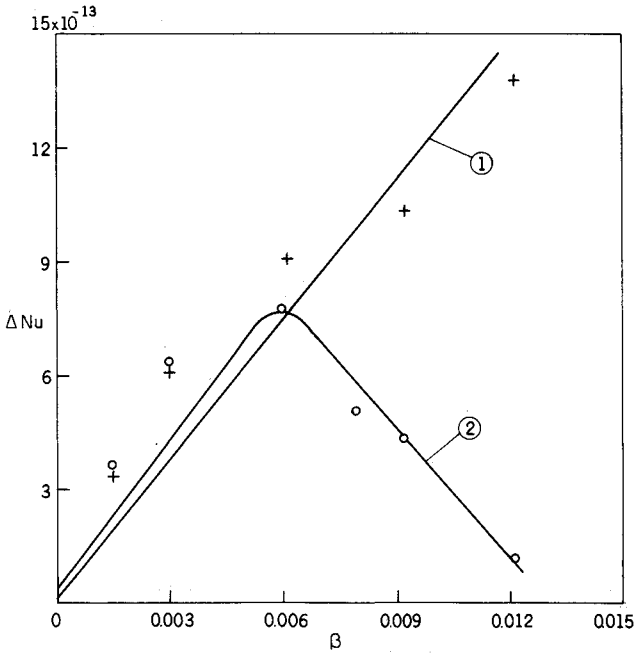

Fig. 5 Effect of particle concentration on heat transfer by particles from a surface [aluminum surface cooled by air and aluminum particles, $d_p = 1$ mm, uniform gas flow, $U_0 = 40$ m/s, $\varepsilon = \varepsilon_w = 0.5$, $\eta = \eta_w = 0.8$, simulated time period = 0.0137 s, $\gamma_0 = 90$ deg].

down more rapidly by the gas and, thus, the effect of interparticle collisions is mitigated.

Augmentation of heat transfer by adding solid particles to a gas stream has been studied extensively.[10,21,37] Generally, the direct heat-transfer rate from the wall to the solid phase is rather low because of the small contact area and duration of collision between the wall and particles. Nevertheless, in some aeronautical applications, the contribution of the direct-contact heat transfer may become significant, particularly when particles undergo phase change on the wall. It is therefore of interest to study the effect of varying flow parameters on direct-contact heat transfer.

Heat transfer between a wall and a particle-laden jet was studied for aluminum particles impacting on an aluminum surface. For such particles ($d_p = 1$ mm), typical values of t_{col} and A_{12} (for $v_{12} = 20$ m/s, $\theta = 45$ deg, $\varepsilon = 1$) are 4.2×10^{-6} s and 7.2×10^{-9} m^2, respectively. In Fig. 5, the effect of increasing particle load, for equal process durations is studied by calculating for different particle concentrations the particles' contribution to the heat transfer from the surface

$$Nu_s = \frac{q \cdot D}{[k_{air}(T_w - T_{air})\pi D^2/4]} \tag{49}$$

where D is the target surface diameter and q the rate of heat transfer. In the absence of interparticle collisions, the heat transfer is seen to increase linearly with the increase in particle load. When interparticle collisions are taken into account, at low particle concentrations a slight augmentation in heat removal is produced by the collisions. A possible explanation for this augmentation is that at angles of impact smaller than 90 deg and smaller impact velocities, as caused by interparticle collisions, the $A_w \Delta t_w$ are increased considerably [expression (33)]. At higher particle concentrations, however, interparticle collisions cause the heat removal to decrease with increased particle load. This reduction in heat removal rates may be attributed to the screening effect, preventing particles from reaching the surface. Thus, an optimal particle load should be employed to obtain maximal heat removal.

The effect of turbulence on the heat transfer by particles was similar to the effect of turbulence on the erosion, as discussed herein. In turbulent gas flow, particles were swayed away from the surface and hence removed somewhat less heat from the surface. The effect of interparticle collisions exhibited trends similar to those observed in the absence of turbulence, although much weaker. One should note that for higher particle loading ratios, as observed in the cooling of a channel's walls by suspensions flowing inside it,[37] additional changes of the heat-transfer characteristics may be caused by alteration of the gas turbulence characteristics.

References

[1]Laitone, J. A., "Erosion Prediction near a Stagnation Point Resulting from Aerodynamically Entrained Solid Particles," *Journal of Aircraft*, Vol. 16, Oct. 1979, pp. 809–814.

[2]Finnie, I., "Erosion of Surfaces by Solid Particles," *Wear*, Vol. 3, 1960, pp. 87–103.

[3]Laderman, A. J., Lewis, C. H., and Byron, S. R."Two Phase Plume Impinging Effects," *AIAA Journal*, Vol. 8, Oct. 1970, pp. 1831–1839.

[4]Smith, D. H., "Debris Shielding in Regions of High Edge Velocity,"*AIAA Journal*, Vol. 14, Jan. 1976, pp. 94–96.

[5]Smeltzer, C. E., Gulden, M. E., and Compton, W. A., "Mechanisms of Metal Removal by Impacting Dust Particles," *Journal of Basic Engineering, Transactions of ASME*, Vol. 92D, Sept. 1970, pp. 639–654.

[6]Tilly, G. P., "Erosion Caused by Impact of Solid Particles," in *Treatise on Materials Science and Technology*, Vol. 13, edited by D. Scott, Academic, New York, 1979, pp. 287–319.

[7]Uumois, H. and Kleis, I., "A Critical Analysis of Erosion Problems Which Have Been Little Studied," *Wear*, Vol. 31, 1975, pp. 359–371.

[8]Reinecke, W. G., "Debris Shielding During High-Speed Erosion," *AIAA Journal*, Vol. 12, Nov. 1974, pp. 1592–1594.

[9]Soo, S. L., "Dynamic Interactions of Granular Materials," in *Advances in the Mechanics and Flow of Granular Materials*, Vol. 2, edited by M. Shahinpoor, Trans-Tech Publications, New York, 1983, pp. 675–698.

[10]Boothroyd, R. G., *Flowing Gas-Solids Suspensions*, Chapman and Hall, London, 1971.

[11]Pai, S. I., "Fundamental Equations of a Mixture of a Gas and Small Spherical Solid Particles from Simple Kinetic Theory," *Review of Roumanian Science and Technology—Mechanical Applications*, Vol. 19, April 1974, pp. 605–621.

[12]Marble, F. E., "Mechanism of Particle Collision in the One-Dimensional Dynamics of Gas-Particle Mixtures," *Physics of Fluids*, Vol. 7, Aug. 1964, pp. 1270–1282.

[13]Lifshitz, E. M. and Pitaevskii, L. P., *Physical Kinetics*, Pergamon, Oxford, 1981.

[14]Langmuir, I. and Blodget, K., "Mathematical Investigation of Water Droplet Trajectories," *Journal of Meteorology*, Vol. 5, 1948, p. 175.

[15]Jenkins, J. T. and Savage, S. B., "A Theory of the Rapid Flow of Identical, Smooth, Nearly Elastic, Spherical Particles," *Journal of Fluid Mechanics*, Vol. 130, May 1983, pp. 187–202.

[16]Ogawa, S., "On the Statistical Approaches to the Dynamics of Fully Fluidized Granular Materials," in *Advances in the Mechanics and Flow of Granular Materials*, Vol. 2, edited by M. Shahinpoor, Trans-Tech Publications, New York, 1983, pp. 601–612.

[17]Kitron, A., Elperin, T., and Tamir, A., "Monte Carlo Simulation of Gas-Solids Suspension Flows in Impinging Streams Reactors," *Journal of Fluid Mechanics* (submitted for publication).

[18]Gottlieb, J. J. and Coskunses, C. E., "Effects of Particle Volume on the Structure of a Partly Dispersed Normal Shock Wave in a Dusty Gas," Univ. of Toronto, Inst. for Aerospace Studies, Toronto, Canada, UTIAS Rept. 295, 1985.

[19]Bird, G. A., *Molecular Gas Dynamics*, Clarendon, Oxford, 1976.

[20]Soo, S. L., "Net Effect of Pressure Gradient on a Sphere," *Physics of Fluids*, Vol. 19, May 1976, p. 757.

[21]Soo, S. L., *Fluid Dynamics of Multiphase Systems*, Blaisdell, Waltham, MA, 1967.

[22]Timoshenko, S. and Goodier, J. N., *Theory of Elasticity*, 2nd ed., McGraw-Hill, New York, 1934, p. 339.

[23]Clift, R., Grace, J. R., and Weber, M. E. *Bubbles, Drops and Particles*, Academic, New York, 1978, p. 112.

[24]Rudinger, G., *Fundamentals of Gas-Particles Flow*, Elsevier, Amsterdam, 1980, pp. 16–17.

[25]Bitter, J. G. A., " A Study of Erosion Phenomena. Part 2," *Wear*, Vol. 6, May/June 1963, pp. 169–190.

[26]Grant, G. and Tabakoff, W., "Erosion Prediction in Turbomachinery Resulting from Environmental Solid Particles," *Journal of*

Aircraft, Vol. 12, May 1975, pp. 471–478.

[27]Wakeman, T. and Tabakoff, W., "Erosion Behavior in a Simulated Jet Engine Environment," *Journal of Aircraft*, Vol. 16, Dec. 1979, pp. 828–833.

[28]Tabakoff, A., Hamed, A., and Beacher, B., "Investigation of Gas Particle Flow in an Erosion Wind Channel," *Wear*, Vol. 86, April 1983, pp. 73–88.

[29]Dunbar, L. E., Courtney, J. F., and McMillen, L. D., "Heating Augmentation in Erosive Hypersonic Environments," *AIAA Journal*, Vol. 13, July 1975, pp. 908–912.

[30]Donaldson, C. D. and Snedecker, R. S., "A Study of Free Jet Impingement. Part 1. Mean Properties of Free and Impinging Jets," *Journal of Fluid Mechanics*, Vol. 45, Jan. 1971, pp. 281–319.

[31]Donaldson, C. D., Snedecker, R. S., and Margolis, D. P., "A Study of Free Jet Impingement. Part 2. Free Jet Turbulent Structure and Impingement Heat Transfer," *Journal of Fluid Mechanics*, Vol. 45, 1971, pp. 477–512.

[32]Yoshida, H. and Masuda, H., "Model Simulation of Particle Motion in Turbulent Gas-Solid Pipe Flow," *Powder Technology*, Vol. 26, 1980, pp. 217–220.

[33]Giralt, F., Chia, C. J., and Trass, O., "Characterization of the Impingement Region in an Axisymmetric Turbulent Jet," *Industrial Engineering Chemistry Fundamentals*, Vol. 6, Feb. 1977, pp. 21–25.

[34]Melville, W. K. and Bray, K. N. C., " A Model of the Two Phase Turbulent Jet," *International Journal of Heat and Mass Transfer*, Vol. 22, May 1979, pp. 647–656.

[35]Abrahamson, J., "Collision Rates of Small Particles in a Vigorously Turbulent Fluid," *Chemical Engineering Science*, Vol. 30, Nov. 1975, pp. 1371–1379.

[36]Shuen, J. S., Chen, L. D., and Faeth, G. M., "Predictions of the Structure of Turbulent, Particle-Laden Round Jets," *AIAA Journal*, Vol. 21, Nov. 1983, pp. 1483–1484.

[37]Depew, C. A. and Kramer, T. J., "Heat Transfer to Flowing Gas-Solid Mixtures", in *Advances in Heat Transfer*, edited by J. P. Hartnett and T. F. Irving, Jr., Vol. 9, Academic, New York, pp. 113–180.